Analyst

Accepted Manuscript

This article can be cited before page numbers have been issued, to do this please use: J. Lin, Q. Wang, X. Wang, Y. Zhu, X. Zhou and H. Wei, *Analyst*, 2020, DOI: 10.1039/D0AN00451K.

ROYAL SOCIETY OF CHEMISTRY

rsc.li/analyst

DOI: 10.1039/D0AN00451K

Gold Alloy-Based Nanozyme Sensor Arrays for Biothiols Detection

Junshu Lin,[1,2] Quan Wang,[2] Xiaoyu Wang,[2] Yunyao Zhu,[2] Xi Zhou,[1,*] and Hui Wei[1,2,3,*]

[1]Department of Biomaterials, College of Materials, Xiamen University, Xiamen, Fujian 361005, China.

[2]Department of Biomedical Engineering, College of Engineering and Applied Sciences, Nanjing National Laboratory of Microstructures, Jiangsu Key Laboratory of Artificial Functional Materials, Chemistry and Biomedicine Innovation Center (ChemBIC), Nanjing University, Nanjing, Jiangsu 210093, China.

[3]State Key Laboratory of Analytical Chemistry for Life Science and State Key Laboratory of Coordination Chemistry, School of Chemistry and Chemical Engineering, Collaborative Innovation Center of Chemistry for Life Sciences, Nanjing University, Nanjing, Jiangsu 210023, China.

Email: xizhou@xmu.edu.cn; weihui@nju.edu.cn; Web: http://weilab.nju.edu.cn; **Tel:** +86-25-83593272; **Fax:** +86-25-83594648.

Abstract Biothiols play an important role in living cells and are associated with many diseases. Thus, it is necessary to develop a facile, cost-effective, and convenient analytical method for detection of biothiols. Nanozymes are functional nanomaterials with enzymatic activities. Due to their unique advantages (*e.g.*, low cost, high stability, and multifunctionality), nanozymes have been extensively used to construct sensing systems. Previous studies demonstrated colorimetric assays for biothiols detection because they could competitively inhibit the peroxidase-like activities of nanozymes. However, few studies were able to differentiate biothiols from each other. To address these challenges, herein, we first synthesized Au alloy nanozymes with better peroxidase-like activities than gold nanoparticles (AuNPs). Then, cross-reactive sensor arrays were constructed with three alloy nanozymes. Six typical biothiols (i.e.,

glutathione, cysteine, dithiothreitol, mercaptoacetic acid, mercaptoethanol, and mercaptosuccinic acid) were successfully detected and discriminated by the as-prepared nanozyme sensor arrays. Moreover, the practical application of the nanozyme sensor arrays was demonstrated by discriminating biothiols in serum successfully.

Keywords: Nanozymes, Peroxidase mimics, Sensor arrays, Gold-based alloys, Biothiols detection

Introduction

Biothiols are important components of many proteins and bioactive small molecules which are maintaining the redox homeostasis in biological systems.[1, 2] Altering the level of cellular biothiols can be linked to a number of diseases. For example, an imbalance of glutathione (GSH) and cysteine (Cys) can lead to Alzheimer's disease, cancer, and other diseases.[3-5] Dithiothreitol (DTT) has an effect on some oxygen catalytic reactions.[6] Mercaptoacetic acid (MA) is involved in genotoxicity and may cause distortion.[7] Mercaptoethanol (ME) can effectively enhance the immune function of lymphocytes.[8] Mercaptosuccinic acid (MS) has antihypertensive effect.[9] Some biothiols, such as GSH and Cys, have similar structures and reactivities. Therefore, it is necessary to develop facile, sensitive, and selective methods for biothiol detection. A number of methods have been applied to detect biothiols, including fluorescent assays,[10-13] mass spectrometry (MS),[14] capillary electrophoresis (CE),[15] and high-performance liquid chromatography (HPLC), *etc*.[16] While these methods have shown good analytical performance for individual biothiols, HPLC and CE are highly cost and complicated to operate. Others are unable to distinguish multiple biothiols simultaneously. Sensor arrays (also called artificial noses/tongues) are powerful sensing platforms for multiplex detection, which are based on the cross-reaction between the sensing components and multiple analytes. The generated multi-channel signals are converted into certain patterns to distinguish a variety of analytes.[17-24] To enable the multiplex detection of biothiols, several fluorescence sensor arrays were developed for biothiol assays.[25-27] Nevertheless, the fluorophores are complicated to be

synthesized and can be photo-bleached, which limited their practical applications. Here we proposed to use nanozyme sensor arrays for biothiol detection, which are more facile to be fabricated and more stable. Moreover, compared with fluorescent sensor arrays, they can provide catalytically amplified signals.

Nanozymes are nanomaterials with enzymatic activities.[28, 29] Compared with natural enzymes, nanozymes have favorable stability and cost-effectiveness and can be used under harsh conditions. Since the discovery of peroxidase-like Fe_3O_4 nanoparticles (NPs) in 2007,[30] a variety of nanomaterials have been exploited to mimic various natural enzymes.[31-36] Among them, many noble metal nanomaterials have been reported as peroxidase mimics, such as Au,[37-41] Pt,[42-46] Ru,[47] and Pd.[48, 49] They have been widely used for biomedical detection and therapy. Recently, researchers showed that the peroxidase-like activities of noble metal nanozymes could be intentionally modulated by using biothiols. For example, L-cysteine and homocysteine could effectively inhibit the catalytic oxidation of 3,3',5,5'-tetramethylbenzidine (TMB) with Au_xPt_y alloy nanozyme in the presence of H_2O_2.[50] In our recent work, we constructed sensor arrays by using peroxidase-like Pt, Ru, and Ir nanozymes to detect versatile analytes including biothiols.[51] Compared with individual metal, bimetallic and trimetallic NPs can transfer electronic charge to adjacent metal atoms. Thus, noble metal alloys usually possess higher catalytic activities.[52] We reasoned that the metal alloys-based nanozymes would also possess higher peroxidase-like activities. To demonstrate our hypothesis, in this work we synthesized three AuNPs-based alloys and used them to fabricate nanozyme sensor arrays for thiol detection. AuNPs were chosen due to their unique size-dependent electronic, chemical, optical, and catalytic properties.[53-56] We synthesized three gold-based alloys, AuPt, AuPd, and AuPtRu. They all exhibited enhanced peroxidase-like activities compared with monometallic noble metal nanozymes. Since the peroxidase-like activities of these gold-based alloys could be modulated by biothiols, we constructed sensor arrays to detect six typical biothiols based on the three alloy nanozymes. The results showed that the sensor arrays successfully distinguished the six biothiols in a broad concentration range and even in serum samples.

View Article Online
DOI: 10.1039/D0AN00451K

Experimental Section

Chemicals and Materials

Chloroauric acid ($HAuCl_4 \cdot 4H_2O$), chloroplatinic acid ($H_2PtCl_6 \cdot 6H_2O$), and sodium borohydride ($NaBH_4$) were purchased from Sigma-Aldrich. Ruthenium chloride hydrate ($RuCl_3 \cdot xH_2O$), palladium chloride ($PdCl_2$), poly-(vinylpyrrolidone) (PVP, M_w 20000), mercaptoacetic acid (MA), L-cysteine (Cys), mercaptosuccinic acid (MS), dithiothreitol (DTT), and fetal bovine serum (FBS) were purchased from Aladdin Chemical Reagent Co., Ltd. Glutathione (GSH) and mercaptoethanol (ME) were purchased from J&K Scientific. Hydrogen peroxide (H_2O_2), *o*-phenylenediamine (OPD), acetic acid (HOAc), and sodium acetate trihydrate (NaOAc) were purchased from Sinopharm Chemical Reagent Co., Ltd. All aqueous solutions were prepared with deionized water (18.2 MΩ·cm, Millipore).

Instrumentation

Transmission electron microscopy (TEM) imaging was performed on a JEM-2100 microscope at an acceleration voltage of 200 kV (JEOL, Japan). The absorbance of the 96-well plate at 450 nm was collected by a SpectraMax M2e microplate reader (Molecular Devices, USA). UV−visible absorption spectra were collected by using a spectrophotometer (Cary-100, Agilent Technologies). The ζ-potential distribution was measured on a Nanosizer ZS90 (Malvern).

Synthesis of AuPt and AuPd

The AuPt and AuPd were synthesized as follows.[57] To synthesize AuPt, 500 μL of $HAuCl_4 \cdot 4H_2O$ (50 mM), 500 μL of $H_2PtCl_6 \cdot 6H_2O$, and 10 mg of PVP were dissolved in 10 mL of H_2O and stirred for 5 min. Then 4 mL of $NaBH_4$ (2.5 mg/mL) was added and the mixed solution was stirred for another 30 min.

The synthesis method of AuPd was slightly different from AuPt. 2 mg of $PdCl_2$ was dissolved in 10 mL of H_2O and treated with sonication to obtain a clear solution. Then 500 μL of $HAuCl_4 \cdot 4H_2O$ (50 mM) and 10 mg of PVP were added and the mixture was stirred for 5 min. Further, 2 mL of $NaBH_4$ (3 mg/mL) was added into the mixed solution and stirred for another 30 min.

View Article Online
DOI: 10.1039/D0AN00451K

Synthesis of AuPtRu

The AuPtRu alloy was synthesized as follows.[58] 4 mg of $RuCl_3 \cdot xH_2O$, 150 μL of $HAuCl_4 \cdot 4H_2O$ (50 mM), 150 μL of $H_2PtCl_6 \cdot 6H_2O$ (50 mM), and 30 mg of PVP were dissolved in H_2O to reach a final volume to 10 mL and stirred for 5 min. Then 4 mL of ascorbic acid (7.5 mg/mL) was added into the mixed solution and treated with sonication for another 1 h. The product was washed with ethanol for several times and dispersed into deionized water.

Peroxidase-like Activity Measurements

The peroxidase-like activities of the Au alloys were measured by using a peroxidase chromogenic substrate. For AuPd, 50 μL of AuPd solution (100 μg/mL) was added into 950 μL sodium acetate buffer (0.2 M, pH 4.5) containing 10 mM H_2O_2 and 2 mM OPD. For AuPt and AuPtRu, 20 μL of solution (100 μg/mL) was added into 980 μL of sodium acetate buffer (0.2 M, pH 4.5) containing 2 mM OPD and 10 mM H_2O_2. The absorption spectra were measured on a UV−visible spectrophotometer.

Effect of Biothiols on Peroxidase-like Activity

To verify the effect of biothiols on the activities of alloy nanozymes, the alloy solution (5 μg/mL of AuPd, 2 μg/mL of AuPt and AuPtRu) was added into sodium acetate buffer (0.2 M, pH 4.5) with different amounts of biothiols and incubated for 20 min at room temperature. Then a sodium acetate buffer (0.2 M, pH 4.5) containing 10 mM H_2O_2 and 2 mM OPD was added to a final volume of 1 mL. The reaction solution was incubated at 37 ºC for another 20 min and the absorption spectra were measured.

Biothiols Discrimination

In a 96-well plate, a 5 × 7 region was selected in which the blank and six biothiols occupied a 5-well row. Briefly, 70 μL of sodium acetate buffer (0.2 M, pH 4.5) containing nanozymes and biothiols was added into each well and incubated for 20 min at room temperature. The concentrations of AuPd, AuPt and AuPtRu alloys were 5, 2, and 2 μg/mL, respectively. Then another 10 μL of H_2O_2 (100 mM) and 20 μL of OPD (10 mM) were quickly added into each well to a final volume of 100 μL. The absorbance was measured by a microplate reader after 20 min incubation at 37 ºC. Moreover, the six biothiols were tested against the three nanozymes five times each to

give a training-data matrix of 6 biothiols × 3 arrays × 5 replicates. The data were processed by linear discriminant analysis.

Results and Discussion

Synthesis and Characterization of Au Alloy-Based Nanozymes

Transmission electron microscopy (TEM) imaging was applied to confirm the successful synthesis of AuPd, AuPt, and AuPtRu. As shown in Figure 1a-c, AuPd, AuPt, and AuPtRu with average sizes of 5, 4, and 200 nm were obtained, respectively. Zeta potential measurement indicated that all the three nanozymes were negatively charged (Figure S1). After the successful synthesis of AuPd, AuPt, and AuPtRu, we measured their peroxidase-like activities by using a chromogenic substrate of OPD. The generated OPD oxidation product (oxOPD) had an absorption peak at around 450 nm. As shown in Figure S2, after incubated for 1 min, all the three nanozymes had a strong absorption peak at 450 nm. Similar to natural enzymes, the peroxidase-like activities of the nanozymes were also pH-dependent (Figure S3c). Different from natural enzymes, the activities of the alloy nanozymes increased gradually as the temperature increasing (Figure S3d). Moreover, all the alloy nanozymes exhibited higher peroxidase-like activities than the corresponding monometallic noble metal nanozymes (Figure S4), demonstrating the advantages of the alloy strategy for designing nanozymes.

Then we evaluated the effects of biothiols on the peroxidase-like activities of the alloy nanozymes. We selected six typical biothiols including GSH, Cys, DTT, MS, ME, and MA. Taking Cys as an example, the absorbance at 450 nm decreased gradually as the increasing concentration of Cys, suggesting that Cys exhibited concentration-dependent inhibition of the catalytic activities of the three nanozymes (Figure 1d-f). In addition, all the six biothiols also exhibited obvious inhibition on the activities of the three nanozymes (Figures 2 and S5-S9).

Nanozyme Sensor Arrays for Biothiols

To verify the sensing capability, the sensor arrays were first used to discriminate the six biothiols in different concentrations. As shown in Figure 3, GSH, Cys, DTT, and MS at concentrations varying from 1 to 1000 μM were well discriminated. As MA and

ME exhibited stronger inhibition on the peroxidase-like activities of Au alloy nanozymes (Figures S5-S9), 1 to 50 μM of MA and ME were analyzed. As shown in Figure 3c and 3f, both of MA and ME were also well discriminated by using the sensor arrays.

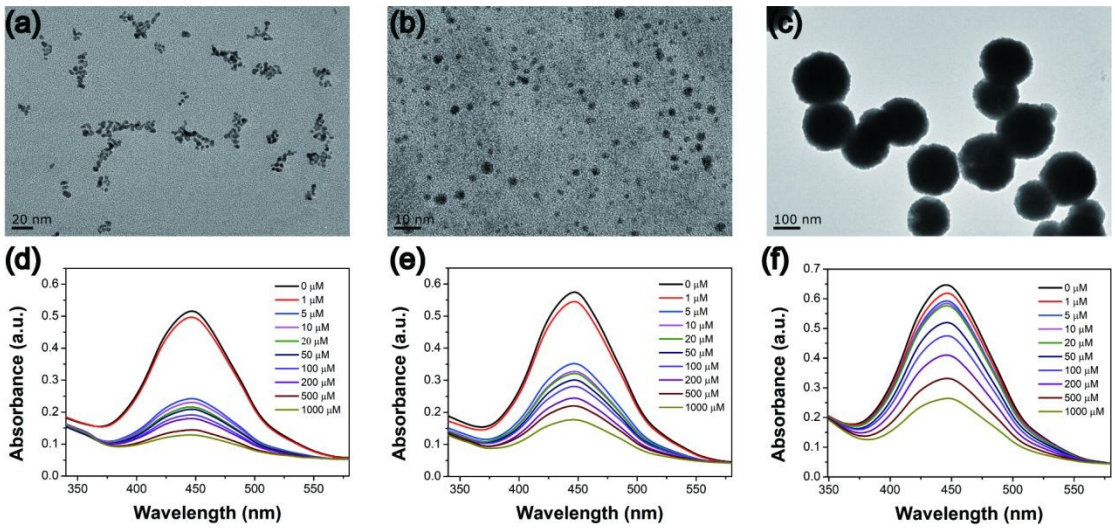

Figure 1. (a-c) TEM images of AuPd, AuPt, and AuPtRu nanozymes. (d-f) Typical absorption spectra for monitoring the catalytic oxidation of OPD in the presence of (d) AuPd, (e) AuPt, and (f) AuPtRu nanozymes with various concentrations of Cys.

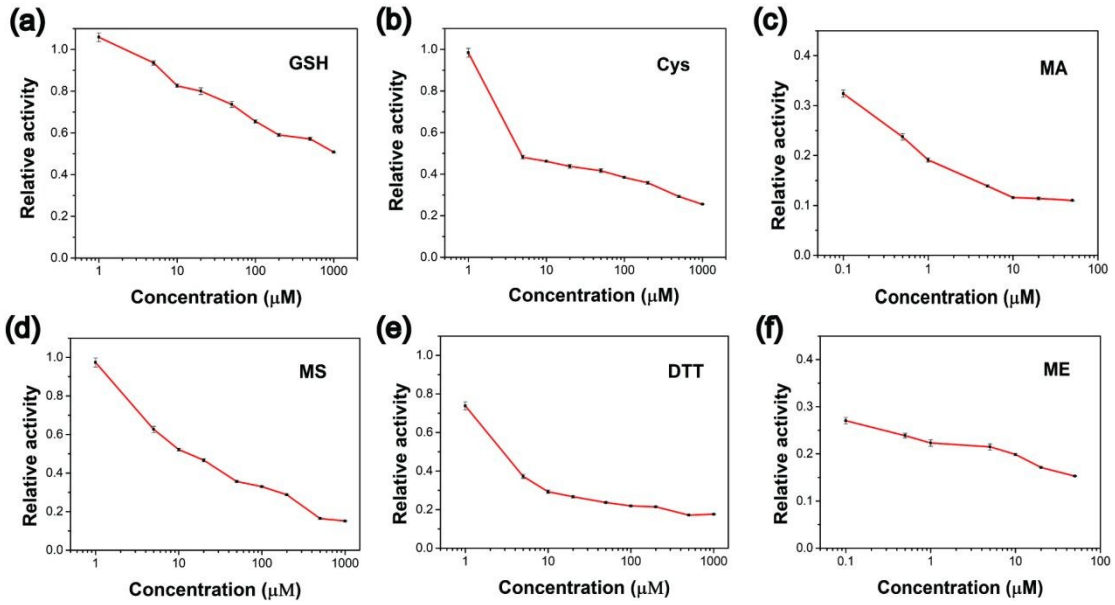

Figure 2. Normalized peroxidase-like activity of AuPd nanozyme after incubation with different concentrations of (a) GSH, (b) Cys, (c) MA, (d) MS, (e) DTT, and (f) ME. Each error bar shows the standard deviation of five independent measurements.

Because the six biothiols exhibited different competitive inhibition for each nanozyme, colorimetric sensor arrays for these biothiols were established. Taking 5 μM

biothiols as an example, they were incubated with the three alloy nanozymes for a period of time in the presence of H_2O_2 and OPD in a well plate. After the incubation, the absorbance at 450 nm was recorded by using a microplate reader. $(A_0\text{-}A)/A_0$ was used to characterize the inhibition of biothiols on the peroxidase-like activities of nanozymes, where A was the absorbance at 450 nm of oxOPD in the presence of biothiols in the nanozymes reaction system, and A_0 was that of the reaction system without biothiols (Figure S10). In order to show the results more intuitively, we applied linear discriminant analysis (LDA) to convert the training matrix (3 alloy nanozymes × 6 biothiols × 5 repetitive units) into three canonical scores, and the first two important discrimination factors were used to generate a 2D canonical score plot. To further verify the ability of the sensor arrays to distinguish biothiols, as shown in Figures 4a and S11, we set five different concentrations from 1 to 50 μM (1, 5, 10, 20, and 50 μM). For all of them, well distinguished patterns were obtained. These results demonstrated the alloy nanozyme-based sensor arrays could efficiently discriminate six biothiols ranging from 1 to 50 μM.

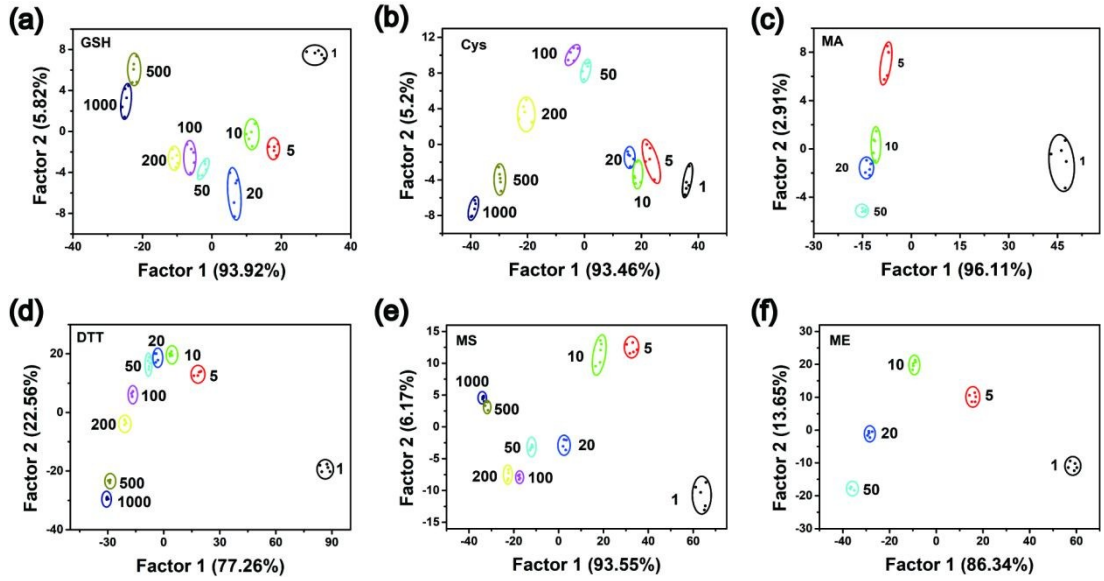

Figure 3. 2D canonical score plots for the first two factors of response patterns obtained against different concentrations (μM) of (a) GSH, (b) Cys, (c) MA, (d) DTT, (e) MS, and (f) ME.

We further assessed the application of the sensor arrays to discriminate the biothiol mixtures. GSH and Cys with different molar ratios at a total concentration of 20 μM were prepared and analyzed. As shown in Figure 4b, the mixtures with different ratios were clustered into five groups. The mixtures of GSH and DTT with different ratios

were also well discriminated (Figure 4c). These results validated the capacity of the alloy nanozyme-based sensor arrays to discriminate biothiols mixtures.

Practical Applications of Nanozyme Sensor Arrays.

To demonstrate the potential practical applications of the nanozyme sensor arrays, the biothiols in serum were tested. Here, fetal bovine serum (FBS) was taken as an example to investigate the practical discrimination ability of sensor arrays. First, the response patterns of 50 μM biothiols in 1% FBS were measured and analyzed by LDA. As shown in Figure 4d, the sensor arrays exhibited a good discrimination for the six biothiols in the presence of FBS. Then the biothiols with lower concentrations of 20 and 10 μM in 1% FBS were measured (Figure 4e-f). All the six biothiols were well discriminated and clustered into distinct groups with no overlap. These results showed that the sensor arrays successfully discriminated the six biothiols in relatively complicated biological fluids, indicating the potential of practical applications.

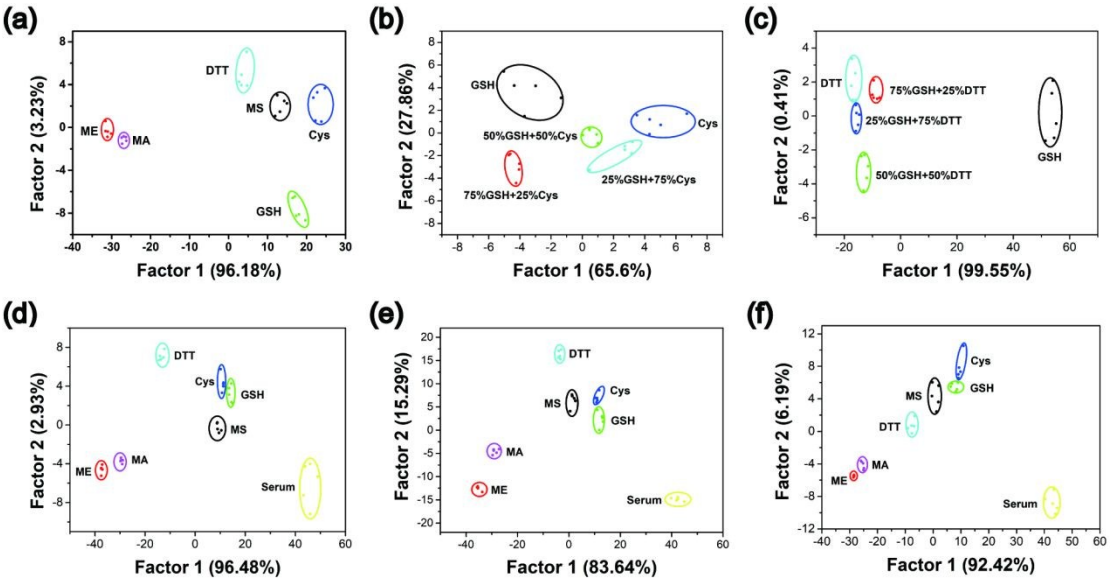

Figure 4. 2D canonical score plots for the first two factors of the colorimetric response patterns obtained against (a) 1 μM biothiols. (b-c) 2D canonical score plots for the first two factors of the colorimetric response patterns obtained against mixtures of (b) GSH and Cys, (c) GSH and DTT at different molar ratios (total concentration at 20 μM). (d-f) 2D canonical score plots for the first two factors of the colorimetric response patterns obtained against (d) 50 μM, (e) 20 μM, and (f) 10 μM of biothiols in the presence of 1% FBS.

Conclusions

In summary, three peroxidase-like gold-based alloys were successfully synthesized and they all exhibited excellent catalytic activities. Moreover, they showed higher

peroxidase-like activities compared with the corresponding single noble metal nanozymes, demonstrating the advantages of the alloy strategy for design of new nanozymes. On the basis of the competitive inhibition to peroxidase-like activities of gold-based alloys by biothiols, sensor arrays were constructed to discriminate six typical biothiols. The sensor arrays showed great discrimination towards six biothiols. Moreover, the fabricated sensor arrays were successfully applied both in aqueous solutions and serum samples. This work not only provides a facile and sensitive method to discriminate biothiols but also broadens the applications of nanozymes in sensor arrays. We also noted that the current sensor arrays may not be applicable to real samples (such as whole blood samples). Thus, further efforts are needed to fulfill the promise of nanozyme sensor arrays in future studies.

Acknowledgements

This work was supported by National Natural Science Foundation of China (21722503 and 21874067), PAPD Program, Open Funds of the State Key Laboratory of Analytical Chemistry for Life Science (SKLACLS1704), Open Funds of the State Key Laboratory of Coordination Chemistry (SKLCC1819), and Fundamental Research Funds for the Central Universities (21314380145).

References

1. E. Weerapana, C. Wang, G. M. Simon, F. Richter, S. Khare, M. B. Dillon, D. A. Bachovchin, K. Mowen, D. Baker and B. F. Cravatt, *Nature*, 2010, **468**, 790-795.
2. C. Y. Chen, W. Liu, C. Xu and W. S. Liu, *Biosens. Bioelectron.*, 2016, **85**, 46-52.
3. J. Lu, E. H. Chew and A. Holmgren, *Proc. Natl. Acad. Sci.*, 2007, **104**, 12288-12293.
4. S. Seshadri, A. Beiser, J. Selhub, P. F. Jacques, I. H. Rosenberg, R. B. D'Agostino, P. W. Wilson and P. A. Wolf, *New Engl. J. Med.*, 2002, **346**, 476-483.
5. G. Y. Wu, Y. Z. Fang, S. Yang, J. R. Lupton and N. D. Turner, *J. Nutr.*, 2003, **134**, 489-492.
6. K. Kim, S. G. Rhee and E. R. Stadtman, *J. Biol. Chem.*, 1985, **260**, 15394-15397.
7. S. A. Jewell, G. Bellomo, H. Thor, S. Orrenius and M. Smith, *Science*, 1982, **217**, 1257-1259.
8. M. L. Heidrick, L. C. Hendricks and D. E. Cook, *Mech. Ageing Dev.*, 1984, **27**, 341-358.
9. S. Chong and H. L. Fung, *Biochem. Pharmacol.*, 1991, **42**, 1433-1439.
10. X. Xia and Y. Qian, *Analyst*, 2018, **143**, 5218-5224.
11. S. Mandani, B. Sharma, D. Dey and T. K. Sarma, *Nanoscale*, 2015, **7**, 1802-1808.
12. L. Y. Niu, Y. Z. Chen, H. R. Zheng, L. Z. Wu, C. H. Tung and Q. Z. Yang, *Chem. Soc. Rev.*, 2015, **44**, 6143-6160.
13. X. Zhang, Y. C. Yan, Y. D. Hang, J. Wang, J. L. Hua and H. Tian, *Chem. Commun.*, 2017, **53**, 5760-5763.

14. G. S. Sarela, B. Susanna, D. Alba, A. Jose, M. Henrik and H. Elena, *Nat. Protoc.*, 2014, **9**, 1131-1145.
15. R. Chand, S. K. Jha, K. Islam, D. Han, I. S. Shin and Y. S. Kim, *Biosens. Bioelectron.*, 2013, **40**, 362-367.
16. M. Isokawa, T. Funatsu and M. Tsunoda, *Analyst*, 2013, **138**, 3802-3808.
17. N. D. B. Le, G. Yesilbag Tonga, R. Mout, S. T. Kim, M. E. Wille, S. Rana, K. A. Dunphy, D. J. Jerry, M. Yazdani, R. Ramanathan, C. M. Rotello and V. M. Rotello, *J. Am. Chem. Soc.*, 2017, **139**, 8008-8012.
18. Y. Zhou, W. Huang and Y. He, *Sens. Actuators B Chem.*, 2018, **270**, 187-191.
19. N. A. Rakow and K. S. Suslick, *Nature*, 2000, **406**, 710-713.
20. Y. Geng, W. J. Peveler and V. M. Rotello, *Angew. Chem. Int. Ed.*, 2019, **58**, 5190-5200.
21. J. Hatai, L. Motiei and D. Margulies, *J. Am. Chem. Soc.*, 2017, **139**, 2136-2139.
22. H. Qiu, F. Pu, X. Ran, C. Q. Liu, J. S. Ren and X. G. Qu, *Anal. Chem.*, 2018, **90**, 11775-11779.
23. X. N. Li, F. Wen, B. Creran, Y. D. Jeong, X. R. Zhang and V. M. Rotello, *Small*, 2012, **8**, 3589-3592.
24. X. Y. Wang, L. Qin, M. J. Lin, H. Xing and H. Wei, *Anal. Chem.*, 2019, **91**, 10648-10656.
25. S. Chen, C. H. Xu, Y. L. Yu and J. H. Wang, *Sens. Actuators B Chem.*, 2018, **266**, 553-560.
26. H. Y. Xi, X. Li, Q. Y. Liu and Z. B. Chen, *Anal. Chim. Acta*, 2019, **1051**, 147-152.
27. Y. P. Wu, X. Liu, Q. H. Wu, J. Yi and G. L. Zhang, *Anal. Chem.*, 2017, **89**, 7084-7089.
28. H. Wei and E. K. Wang, *Chem. Soc. Rev.*, 2013, **42**, 6060-6093.
29. J. J. X. Wu, X. Y. Wang, Q. Wang, Z. P. Lou, S. R. Li, Y. Y. Zhu, L. Qin and H. Wei, *Chem. Soc. Rev.*, 2019, **48**, 1004-1076.
30. L. Z. Gao, J. Zhuang, L. Nie, J. B. Zhang, Y. Zhang, N. Gu, T. H. Wang, J. Feng, D. L. Yang, S. Perrett and X. Y. Yan, *Nat. Nanotechnol.*, 2007, **2**, 577-583.
31. Q. Q. Wang, X. P. Zhang, L. Huang, Z. Q. Zhang and S. J. Dong, *ACS Appl. Mater. Interfaces*, 2017, **9**, 7465-7471.
32. Z. Xi, X. Cheng, Z. Q. Gao, M. J. Wang, T. Cai, M. Muzzio, E. Davidson, O. Chen, Y. Jung, S. H. Sun, Y. Xu and X. H. Xia, *Nano Lett.*, 2020, **20**, 272-277.
33. K. L. Fan, H. Wang, J. Q. Xi, Q. Liu, X. Q. Meng, D. M. Duan, L. Z. Gao and X. Y. Yan, *Chem. Commun.*, 2016, **53**, 424-427.
34. Z. J. Zhang, X. H. Zhang, B. W. Liu and J. W. Liu, *J. Am. Chem. Soc.*, 2017, **139**, 5412-5419.
35. Y. Y. Huang, J. S. Ren and X. G. Qu, *Chem. Rev.*, 2019, **119**, 4357-4412.
36. X. Y. Wang, X. J. Gao, L. Qin, C. D. Wang, L. Song, Y. N. Zhou, G. Y. Zhu, W. Cao, S. S. Lin, L. Q. Zhou, K. Wang, H. G. Zhang, Z. Jin, P. Wang, X. F. Gao and H. Wei, *Nat. Commun.*, 2019, **10**, 704.
37. X. Jiang, C. J. Sun, Y. Guo, G. J. Nie and L. Xu, *Biosens. Bioelectron.*, 2015, **64**, 165-170.
38. P. Weerathunge, R. Ramanathan, R. Shukla, T. K. Sharma and V. Bansal, *Anal. Chem.*, 2014, **86**, 11937-11941.
39. Y. Tao, E. G. Ju, J. S. Ren and X. G. Qu, *Adv. Mater.*, 2015, **27**, 1097-1104.
40. M. Y. Kuo, C. F. Hsiao, Y. H. Chiu, T. H. Lai, M. J. Fang, J. Y. Wu, J. W. Chen, C. L. Wu, K. H. Wei, H. C. Lin and Y. J. Hsu, *Appl. Catal., B*, 2019, **242**, 499-506.
41. W. J. Wang, Y. H. Wu, X. L. Lin, W. Chen, A. L. Liu and H. P. Peng, *Chinese J. Anal. Chem.*, 2018, **46**, 1545-1551.
42. Y. Ju and J. Kim, *Chem. Commun.*, 2015, **51**, 13752-13755.

View Article Online
DOI: 10.1039/D0AN00451K

43. Y. Liu, H. Wu, M. Li, J. J. Yin and Z. Nie, *Nanoscale*, 2014, **6**, 11904-11910.
44. G. W. Wu, S. B. He, H. P. Peng, H. H. Deng, A. L. Liu, X. H. Lin, X. H. Xia and W. Chen, *Anal. Chem.*, 2014, **86**, 10955-10960.
45. L. H. Jin, Z. Meng, Y. Q. Zhang, S. J. Cai, Z. H. Zhang, C. Li, L. Shang and Y. H. Shen, *ACS Appl. Mater. Interfaces*, 2017, **9**, 10027-10033.
46. X. H. Wang, Q. S. Han, S. F. Cai, T. Wang, C. Qi, R. Yang and C. Wang, *Analyst*, 2017, **142**, 2500-2506.
47. L. He, Y. Li, Q. Wu, D. M. Wang, C. M. Li, C. Z. Huang and Y. F. Li, *ACS Appl. Mater. Interfaces*, 2019, **11**, 29158-29166.
48. J. M. Lan, W. M. Xu, Q. P. Wan, X. Zhang, J. Lin, J. H. Chen and J. Z. Chen, *Anal. Chim. Acta*, 2014, **825**, 63-68.
49. Y. Liu, D. L. Purich, C. C. Wu, Y. Wu, T. Chen, C. Cui, L. Q. Zhang, S. Cansiz, W. J. Hou, Y. Y. Wang, S. Y. Yang and W. H. Tan, *J. Am. Chem. Soc.*, 2015, **137**, 14952-14958.
50. Y. H. Sun, J. Wang, W. Li, J. L. Zhang, Y. D. Zhang and Y. Fu, *Biosens. Bioelectron.*, 2015, **74**, 1038-1046.
51. X. Y. Wang, L. Qin, M. Zhou, Z. P. Lou and H. Wei, *Anal. Chem.*, 2018, **90**, 11696-11702.
52. H. J. Zhang, M. Okumura and N. Toshima, *J. Phys. Chem. C*, 2011, **115**, 14883-14891.
53. M. C. Daniel and D. Astruc, *Chem. Rev.*, 2004, **104**, 293-346.
54. K. Saha, S. S. Agasti, C. Kim, X. N. Li and V. M. Rotello, *Chem. Rev.*, 2012, **112**, 2739-2779.
55. Y. H. Hu, H. J. Cheng, X. Z. Zhao, J. J. X. Wu, F. Muhammad, S. S. Lin, J. He, L. Q. Zhou, C. P. Zhang, Y. Deng, P. Wang, Z. Y. Zhou, S. M. Nie and H. Wei, *ACS Nano*, 2017, **11**, 5558-5566.
56. S. H. Guo, X. H. Li, J. M. Zhu, T. T. Tong and B. Q. Wei, *Small*, 2016, **12**, 5692-5701.
57. M. Comotti, C. Della Pina and M. Rossi, *J. Mol. Catal. A: Chem.*, 2006, **251**, 89-92.
58. Y. T. Shi, H. Xu, J. Wang, S. M. Li, Z. P. Xiong, B. Yan, C. Q. Wang and Y. K. Du, *Sens. Actuators B Chem.*, 2018, **272**, 135-138.

View Article Online
DOI: 10.1039/D0AN00451K

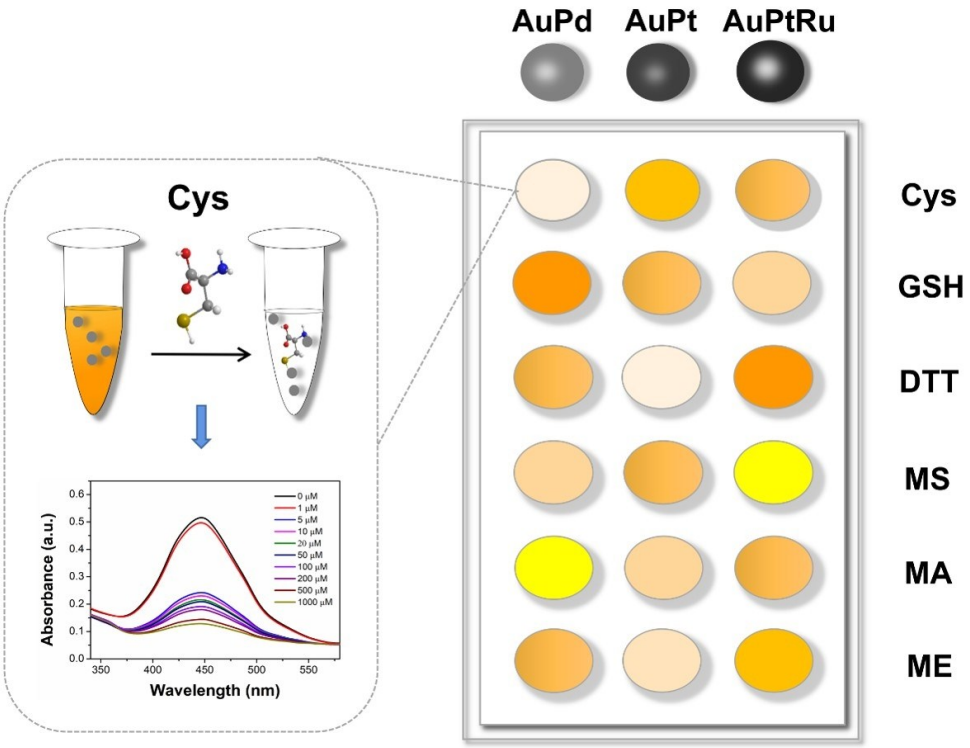

250x190mm (123 x 123 DPI)